This is a preprint of an article published in New Phytologist. The final authenticated version is available online at: https://doi.org/10.1111/nph.18366

Field and saccharification performances of poplars severely downregulated in *CAD1*

Barbara De Meester[1,2], Rebecca Van Acker[1,2], Marlies Wouters[1,2], Silvia Traversari[3,4], Marijke Steenackers[5], Jenny Neukermans[1,2], Frank Van Breusegem[1,2], Annabelle Déjardin[6], Gilles Pilate[6], and Wout Boerjan[1,2*]

[1]Department of Plant Biotechnology and Bioinformatics, Ghent University, Technologiepark 71, 9052 Ghent, Belgium; [2]VIB Center for Plant Systems Biology, Technologiepark 71, 9052 Ghent, Belgium; [3]BioLabs, Institute of Life Sciences, Scuola Superiore Sant'Anna, Piazza Martiri della Libertà 33, 56127, Pisa, Italy (previous affiliation); [4]Research Institute on Terrestrial Ecosytems (IRET-CNR), Via Moruzzi 1, 56124, Pisa, Italy (current affiliation); [5]Research Institute for Nature and Forest (INBO), Gaverstraat 4, Geraardsbergen, Belgium; [6]INRAE, ONF, BioForA Orléans, 2163 Avenue de la pomme de pin, 45075 Ardon, France

Author for correspondence:
Wout Boerjan
Tel: +32 (0)9 33 13 881
Email: wout.boerjan@psb.vib-ugent.be

SUMMARY

- **Lignin is one of the main factors causing lignocellulosic biomass recalcitrance to enzymatic hydrolysis. Greenhouse-grown poplars severely downregulated for *CINNAMYL ALCOHOL DEHYDROGENASE 1* (*CAD1*), the enzyme catalyzing the last step in the monolignol-specific branch of lignin biosynthesis, have increased saccharification yields and normal growth.**
- **Here, we assess the performance of these *hpCAD* poplars in the field under short rotation coppice culture for two consecutive rotations of one and three years.**
- **While one-year-old *hpCAD* wood had 10% less lignin, three-year-old *hpCAD* wood had wild-type lignin levels. Because of their altered cell wall composition, including elevated levels of cinnamaldehydes, both one- and three-year-old *hpCAD* wood showed enhanced saccharification yields upon harsh alkaline pretreatments (up to +85% and +77%, respectively). In contrast to previous field trials with poplars less severely downregulated for *CAD*, the *hpCAD* poplars displayed leaning phenotypes, early bud set, early flowering and yield penalties. Moreover, *hpCAD* wood had enlarged vessels, decreased wood density, and reduced relative and free water contents.**
- **Our data show that the phenotypes of CAD-deficient poplars are strongly dependent on the environment and underpin the importance of field trials in translating basic research towards applications.**

KEY WORDS

CAD, field trial, lignin engineering, poplar, saccharification, water content, wood

INTRODUCTION

Currently, fossil resources are still the main feedstock for the production of energy and chemicals. As a consequence of their rapid depletion and the urgent need to decrease greenhouse gas emissions to counter global warming, a shift from today's fossil-based economy towards a bio-based economy is highly needed (B. Vanholme *et al.*, 2013; Marriott *et al.*, 2016; Rinaldi *et al.*, 2016; Schutyser *et al.*, 2018; Fetting, 2020; Singh *et al.*, 2022). In a bio-based economy, lignocellulosic biomass rather than oil is used as feedstock for the production of fuels, chemicals and materials. Wood is an important source of lignocellulosic biomass and is mainly composed of cellulosic and hemicellulosic polysaccharides embedded in a matrix of lignin. Lignin is an aromatic heteropolymer of which the biosynthetic route is rather well described (Freudenberg, 1959; Vanholme *et al.*, 2019). In dicot plants, the amino acid phenylalanine undergoes a series of enzymatic conversions that finally lead to the production of *p*-coumaryl, coniferyl and sinapyl alcohol. After their biosynthesis in the cytoplasm, these monolignols are translocated over the plasma membrane to the cell wall where they are oxidized by peroxidases and/or laccases and subsequently coupled into the growing lignin polymer as *p*-hydroxyphenyl (H), guaiacyl (G) and syringyl (S) units, respectively (Perkins *et al.*, 2019; Ralph *et al.*, 2019; Vermaas *et al.*, 2019). Dependent on the plant species, also several other less abundant units are incorporated in the lignin polymer, such as conifer- and sinapaldehyde and sinapyl-*p*-hydroxybenzoic acid in poplar lignin (Vanholme *et al.*, 2019).

The polymeric sugars in lignocellulosic biomass can be hydrolyzed (by a process called saccharification) into their monosaccharides, which can be subsequently fermented into biofuels and -chemicals. However, lignocellulosic biomass is recalcitrant towards deconstruction mainly because of the presence of lignin that limits the accessibility of the cell wall polysaccharides by the hydrolyzing enzymes (Chen & Dixon, 2007; Van Acker *et al.*, 2013; Gao *et al.*, 2014). To improve saccharification in biomass crops, efforts have focused on altering the lignin amount and/or composition (Pilate *et al.*, 2002; Chen & Dixon, 2007; Eudes *et al.*, 2012; Van Acker *et al.*, 2013; R. Vanholme *et al.*, 2013; Wilkerson *et al.*, 2014; Smith *et al.*, 2015; Mottiar *et al.*, 2016; Sibout *et al.*, 2016; Chanoca *et al.*, 2019; Oyarce *et al.*, 2019; De Meester *et al.*, 2020).

A promising target for lignin engineering is CINNAMYL ALCOHOL DEHYDROGENASE (CAD), an enzyme that catalyzes the last step of the monolignol biosynthesis pathway by reducing the hydroxycinnamaldehydes into their corresponding alcohols. Using *CAD* sense (*SCAD*) and antisense (*ASCAD*) constructs, CAD activity has been moderately reduced in *Populus tremula* x *P. alba* (30% residual CAD activity in the most downregulated lines) (Baucher *et al.*, 1996; Lapierre *et al.*, 1999). When grown in the greenhouse, *SCAD* and *ASCAD* poplars displayed an unaltered or slightly (2-8%) reduced Klason lignin content, an unaltered S/G ratio and the typical enhanced incorporation of hydroxycinnamaldehydes (mainly sinapaldehyde) into the lignin. Moreover, these greenhouse-grown trees with moderate reduction in CAD activity displayed a red coloration of the xylem (albeit not uniformly distributed over the xylem), grew normally and showed an increased Kraft pulping efficiency [Kraft pulping was the first industrially relevant process that was applied to CAD-deficient poplar wood]. More recently, a *CAD1* hairpin (*hpCAD*) RNAi-mediated silencing approach was used to create *P. tremula* x *P. alba* lines that were more strongly reduced in CAD activity (Van Acker *et al.*, 2017). When grown in the greenhouse, these lines had only 15% residual CAD activity, a 10% reduction in Klason lignin, a reduced S/G ratio and a strong increase in sinapaldehyde incorporation into the lignin. The xylem coloration of *hpCAD* lines was dark red and uniform over the whole stem. Despite their severe reduction in CAD activity, the *hpCAD* poplars still showed a normal growth and displayed increases of up to 81% in glucose release and up to 64% in xylose release after saccharification using alkaline pretreatments, making these lines promising for further evaluation in field conditions.

Field trials are an essential step in translating fundamental knowledge generated in the laboratory to conditions closer to industrial exploitation (Pilate *et al.*, 2015). In contrast to greenhouse-grown poplars that grow and develop continuously, field-grown poplars cease growth and set bud in autumn. Moreover, field-grown poplars interact with environmental factors such as soil type, wind, drought, and pathogens. Field trials also allow the trees to be grown and evaluated under relevant agricultural practices, such as short or medium rotation coppice culture that is preferred when trees are cultivated for biomass and bioenergy purposes. Because environmental factors can greatly influence plant performance (reviewed in Chanoca *et al.* (2019) for lignin-engineered trees), it is crucial to study these aspects when translating research results into commercial applications. When *P. tremula* x *P. alba* lines with moderate reduction

in CAD activity (*SCAD* and *ASCAD*) were grown in the field for two and/or four years, they maintained their commercially relevant changes in lignin content and structure, their normal growth and increased pulping performance (Lapierre *et al.*, 1999; Pilate *et al.*, 2002). Moreover, the lignin modifications had no obvious biological or ecological impacts because no differences were observed in the interactions of *ASCAD* poplars with leaf-feeding insects, microbial pathogens, and soil organisms (Pilate *et al.*, 2002).

Given that the *hpCAD* lines were more severely downregulated for *CAD* as compared with *SCAD* and *ASCAD* lines, and given their significant improvements in saccharification efficiency under alkaline pretreatments, we assessed their performance in the field under short rotation coppice (SRC) culture. The biomass yield, wood composition, wood water content, saccharification efficiency and interactions with the environment of *hpCAD* and control wild-type (WT) lines were evaluated for two consecutive rotations of one and three years of growth in the field.

MATERIALS AND METHODS

Field trial set-up

Poplars (*Populus tremula* x *P. alba* clone '717-1B4') downregulated for *PtaCAD1* (Potri.009G095800.1) using a hairpin construct were described before (Van Acker *et al.*, 2017). Three transgenic lines and a WT control line were simultaneously micropropagated in more than 240 clonal replicates and grown in the greenhouse for 6 weeks. In May 2014, transgenic and WT trees were transferred to the field site located in Wetteren, Belgium (50˚58'40" N, 3˚50'13" E), under a field trial authorization (B/BE/13/V1) provided by the Belgian authorities. The field plot was divided in six randomized blocks, each block containing 40 clonal replicates per line (**Fig. S1a**). Hence, in total, 240 plants per line were evaluated. The plantation density was 7393 trees/ha. A detailed plan of the field trial indicating the distances between rows, blocks and individual trees is shown in **Fig. S1b**. The field was surrounded with a border of WT trees to avoid border effects. The latter trees were not included in the experimental analyses. The trees were grown under SRC culture for two consecutive rotations of one and three years. For more details concerning the two growth cycles (first growth cycle from 2014-2015 and second growth cycle from 2015-2018), phenotyping and two harvests (H1 and H2), see **Note S1**.

Stem water relations and xylem anatomy

Prismatic subsamples of stem portions were collected to determine the water content. The bark was separated from the xylem and the samples were weighed to determine the fresh weight (FW). After overnight immersion in MilliQ-H_2O under vacuum, they were weighed to determine the turgor weight (TW), and then dried for 48 h at 105°C to determine the dry weight (DW). Bark and wood relative water contents (RWCs) were calculated as follows: RWC = 100 × (FW-DW)/(TW-DW). Wood moisture content (α, %), basic density (kg m^{-3}), fibre saturation point (α_f, %) and the amount of free water available to support the hydraulic network (α-α_f) were determined as reported in Traversari *et al.* (2018). Wood samples for anatomical observations were placed in 99% ethanol and stored at 4°C. Next, stem sections were cut into transverse sections of 8- to 12-µm thickness using a sliding microtome SM2010 (Leica, Wetzlar, Germany). The sections were stained with a solution of 0.15% Astra Blue and 0.04% Safranin in 2% acetic acid and observed with an Axioskop light microscope (Zeiss, Oberkochen, Germany). Digital images were used to calculate vessel areas and diameters using the ImageJ software (Schneider *et al.*, 2012). Anatomical analyses were conducted on portions of 1 mm^2 for each sample in the wood ring formed during the previous year. The hydraulically weighted vessel diameter (D_H) was calculated according to Sperry and Saliendra (1994) and the theoretical specific xylem hydraulic conductivity ($K_{(S)t}$) was calculated according to Santiago *et al.* (2004) on the basis of Hagen–Poiseuille equation for ideal capillaries assuming a laminar flow.

Cell wall composition

All cell wall analyses (except for the cellulose determination) were performed on purified cell wall residue (CWR), which is obtained after a sequential extraction with water, ethanol, chloroform, and acetone as described (Van Acker *et al.*, 2013).

Lignin content was measured gravimetrically according to a modified mini-Klason procedure essentially described by Ibáñez and Bauer (2014) and modified according to De Meester *et al.* (2020). The general lignin composition and the quantification of the markers for CAD deficiency, conifer- and sinapaldehyde-derived indenes and dithioketals, were determined using thioacidolysis as described by Robinson and Mansfield (2009) for H1 (**Table S1**) and modified as described in **Table S2** for H2. The monomers released upon thioacidolysis were detected with gas chromatography as their trimethylsilyl ether derivatives (**Table S1**, **Table S2**). Response factors for H, G and S units and markers for CAD deficiency were taken from Van Acker *et al.* (2013).

The total amount of alpha-cellulose was quantified essentially as described by Brendel *et al.* (2000) and modified according to Oyarce *et al.* (2019).The amount of hemicelluloses and their composition were analyzed by a TFA-extraction and subsequent alditol-acetate assay as described (Foster *et al.*, 2010; Van Acker *et al.*, 2013).

Saccharification assays

Saccharification assays were performed as described (Van Acker *et al.*, 2016). Alkaline pretreatments with 6.25 mM and 62.5 mM sodium hydroxide were performed at 90˚C for 3 h. To each sample, an enzyme mixture of cellulase (from *Trichoderma reesei*, Sigma Aldrich) and beta-glucosidase (Accellerase BG, DuPont) was added with an activity of 0.20 filter paper unit (FPU)/mL. Glucose release was measured after 2, 6, 24 and 48 h of saccharification and normalized for the amount of CWR. As saccharification assays were performed on the debarked bottom part of the stem (see above), the glucose release per plant was calculated using the weight of the bottom 1 m of the tree as a proxy of the whole stem (and thus not using the weight of the total tree as this also included the bark).

RESULTS

Severe downregulation of *CAD1* affects growth, bud set, flowering time and xylem coloration in field-grown trees

When grown in the greenhouse, *hpCAD* lines had a 10% reduction in Klason lignin, a reduced S/G, a strong increase in sinapaldehyde incorporation into the lignin, an increased saccharification efficiency, and a normal growth and development (Van Acker *et al.*, 2017). To evaluate whether these lines maintained their improved wood processing characteristics and normal growth when grown under relevant agronomic cultivation practices, a field trial was established. The three transgenic lines described by Van Acker *et al.* (2017) – i.e., *hpCAD4*, *hpCAD19* and *hpCAD24* – and their WT control were grown in a field in Belgium that consisted of six randomized blocks, each block consisting of 40 clonally propagated trees of each genotype (**Fig. S1a, b**). The trees were grown under SRC culture: after planting them in May 2014, they grew as a single stem for nine months (first growth cycle) and were harvested for the first time in February 2015 (H1) (**Note S1**). In spring 2015, the coppiced trees re-sprouted, forming

multiple stems per stool. After growing for an additional three years (second growth cycle), the poplars were harvested for a second time in March 2018 (H2) (**Fig. S1c, Note S1**).

Multiple biomass parameters were determined each year (**Table 1**). Both one- and three-year-old *hpCAD* poplars consistently displayed a reduced height, diameter and weight when compared to the WT (**Table 1**). On average, the tree height was reduced by 10% in one-year-old *hpCAD* poplars of the first and second growth cycle, and by 37% in three-year-old *hpCAD* poplars of the second growth cycle. The total tree weight was reduced with, on average, 22% in one-year-old *hpCAD* poplars of the first growth cycle and with, on average, 33% in three-year-old *hpCAD* poplars of the second growth cycle. The reduction in the biomass and diameter of the main stem (i.e., the tallest and thickest stem) of three-year-old *hpCAD* poplars was slightly compensated by an increased diameter of the side stems (i.e., the other stems next to the tallest and highest main stem) (**Table 1**).

LEAF-E is a tool that allows performing non-linear regression modeling on height measurements to extract growth parameters such as maximum growth rate (Voorend *et al.*, 2014). Using this tool, we found that the overall reduction in biomass of *hpCAD* poplars was correlated with an, on average, 8-9% reduction in maximum growth rate in one-year-old *hpCAD* plants of the first and second growth cycle, and an earlier growth arrest (i.e., the date when the tree growth rate dropped to 0 cm/day) of, on average, 11 and 7 days for one-year-old *hpCAD* plants of the first and second growth cycle, respectively (**Table 1**). Correlated with this, one-year-old *hpCAD* poplars of the first and second growth cycle completed their bud set, on average, 1 week earlier than the WT did (**Fig. S2a, b**). Next to early bud set, *hpCAD* poplars also displayed early flowering (**Fig. S2c**). In the second growth cycle, twenty-seven and fifty-five flowers emerged on two- and three-year-old *hpCAD* poplars, respectively, compared to zero and three flowers on two- and three-year-old WT poplars, respectively.

All field-grown one-year-old (first growth cycle) and three-year-old (second growth cycle) *hpCAD* poplars displayed the typical dark red xylem coloration that was uniformly distributed along the debarked stem, indicative of a strong and stable downregulation of *CAD1* (**Fig. 1**). About 9% of *hpCAD4*, 3% of *hpCAD19* and 4% of *hpCAD24* trees from the first growth cycle displayed a clearly visible white zone in the middle of the otherwise dark-red colored xylem. Wood samples of *hpCAD* trees that displayed this white zone were labelled as ‘white patch wood’ (**Fig. 1**). Wood samples

of the remaining *hpCAD* trees from the first growth cycle that did not show this white zone were labeled as 'red wood'. Interestingly, on average, field-grown *hpCAD* poplars of the first growth cycle had a larger leaning angle of the main stem as compared to WT trees (i.e., the stem was leaning along with the main wind direction) (**Fig. 2**). As white patch *hpCAD* trees had a significantly higher leaning angle than red *hpCAD* trees (**Fig. 2**), the presence of this white zone is probably associated with the larger leaning angles. Similarly, also field-grown *hpCAD* poplars of the second growth cycle occupied a larger surface area (i.e., the outer stems were leaning more towards the soil) (**Fig. 2**), but here, this white zone was not visible in the main or side stems of *hpCAD* lines. Interestingly, the weight of the bottom 1 meter of white patch *hpCAD* stems was not significantly different from that of red *hpCAD* stems from H1 (**Table 1**).

Field-grown *hpCAD* poplars display no collapsed vessels but have a reduced water content

To evaluate the morphology of xylem cells in the stem, cross sections of three-year-old stems from H2 were observed via light microscopy after Safranin and Astra Blue staining. The yield penalty of lignin-modified plants is often associated with collapsed vessels (Muro-Villanueva *et al.*, 2019). In contrast, *hpCAD* lines displayed round, open (non-collapsed) vessels (**Fig. S3**). Nevertheless, microscopic analyses revealed that the *hpCAD* poplars had an altered xylem tissue organization when compared to WT plants (**Table 2**). More specifically, the *hpCAD* poplars had an, on average, 14% increase in vessel diameter (as shown by their increased D_H value) and an, on average, 39% larger total vessel area when compared to the WT. As a consequence, the theoretical specific xylem hydraulic conductivity ($K_{S(t)}$) was increased by, on average, 79% in the *hpCAD* lines when compared to the WT.

Because *hpCAD* poplars did not have irregularly-shaped vessels and even had a higher theoretical specific xylem conductivity because of their enlarged vessels, water content analyses were performed, showing that *hpCAD* wood had a different water strategy compared to WT wood (**Table 3**). Regardless of their increased theoretical $K_{S(t)}$, the relative water content (RWC) in wood was strongly decreased (by, on average, 24%) in the *hpCAD* lines compared to the WT. The latter means that *hpCAD* poplars detain less water in their xylem in relation to their maximal capacity, and thus might have reduced water reserves. Nevertheless, the RWC in bark was similar between the *hpCAD* and WT lines. Moreover, related with their increased vessel

diameter, the *hpCAD* poplars had an, on average, 17% decrease in wood basic density when compared to the WT, probably explaining their higher fiber saturation point (α_f). In other words, from the total amount of water that is present in the xylem (= α), a higher percentage is bound to the xylem cell wall in *hpCAD* poplars when compared to WT poplars. Consequently, the *hpCAD* poplars had a strong decrease (by, on average, 32%) in free water available to support the hydraulic network (α-α_f) when compared to the WT.

Field-grown *hpCAD* poplars display no major differences in pathogen and insect susceptibility

As lignin, or its soluble precursors or derivatives thereof, could influence the palatability of leaves to herbivorous insects and the tolerance of trees to pathogens, the biological interactions of *hpCAD* and WT trees were monitored (**Table 4**). The scoring was performed in 2014 (first year of the first growth cycle), and in 2015 and 2017 (first and third year of the second growth cycle). During that time, the *hpCAD* and WT poplars were only affected by *Melampsora populnea* rust infection and herbivorous insects. No other pathogens were observed. No or very subtle differences (that were not consistent over the three *hpCAD* lines) in susceptibility to *Melampsora populnea* rust infection and herbivorous insect damage were observed between WT and *hpCAD* poplars (**Table 4**). Therefore, we conclude that, despite heavily impacting growth and biomass, severe downregulation of *CAD1* has no major effect on the rust and herbivorous insect susceptibility of field-grown poplar.

Severe deficiency in *CAD1* affects lignin and polysaccharide amount and composition in field-grown trees

To evaluate the effect of severe *CAD1* downregulation on the cell wall composition of field-grown trees, cell wall residue (CWR), cellulose content, and hemicellulose and lignin amount and composition of one-year-old (from H1) and three-year-old (from H2) dried, debarked wood were determined.

First, the cell wall composition of one-year-old WT and *hpCAD* red wood from H1 was determined (**Table 5, Table S3**). CWR was prepared by applying a sequential extraction to remove soluble compounds from the stems. When expressed per dry weight, the %CWR of the *hpCAD* lines was equal to that of the WT, except for *hpCAD19,* which showed a small (0.3%) reduction in %CWR. Lignin content was

determined by the Klason procedure allowing determination of the acid-insoluble lignin fraction (referred to as Klason lignin) and the acid-soluble lignin fraction. The Klason lignin amount in all *hpCAD* lines was reduced by, on average, 10% when compared to the WT, while the acid-soluble lignin amount was equal except for *hpCAD19* which showed a 6% increase in acid-soluble lignin amount. The decreased lignin amount of the *hpCAD* lines was accompanied by a minor reduction in cellulose amount of, on average, 3% and a small increase in hemicellulose amount of, on average, 5% in all *hpCAD* lines when compared to the WT. The relative distribution of the main neutral sugars from the amorphous polysaccharides revealed some changes in the *hpCAD* lines when compared to the WT, mainly diminishments in Rha (of, on average, 85%) and Fuc (of, on average, 85%) and a moderate Xyl enrichment (of, on average, 6%) in all *hpCAD* lines. Lignin structure was studied by thioacidolysis, an analytical degradation method that yields lignin-derived monomers from lignin units involved in labile β-*O*-4 bonds. All *hpCAD* lignins released less monomers (H + G + S) when compared to WT lignins, indicative of a lower frequency of β-*O*-4 interunit bonds. The relative frequency of H units was increased by, on average, 57% in all *hpCAD* lines compared to the WT. The S/G ratio was reduced from 2.67 in the WT to, on average, 2.05 in the *hpCAD* lines as a consequence of their increased relative frequency of G units and decreased relative frequency of S units. The abundance of coniferaldehyde-derived dithioketals derived from coniferaldehyde end groups was found to be substantially decreased by, on average, 35% in the lignin of all *hpCAD* lines compared to the WT, while coniferaldehyde-derived indenes released from coniferaldehyde units ether-linked at their β-positions were below the detection limit in all samples. The abundance of sinapaldehyde-derived dithioketals in *hpCAD* lignin was not significantly different from that of WT lignin, except for *hpCAD19*, in which it was increased by 67%. The abundance of sinapaldehyde-derived indenes was increased by, on average, 57-fold in all *hpCAD* lignins compared to WT lignin.

Second, the cell wall composition of one-year-old *hpCAD* white patch wood from H1 was determined (**Table 5, Table S3**). When compared to one-year-old *hpCAD* red wood, one-year-old *hpCAD* white patch wood displayed an equal amount of CWR per dry weight, a similar amount of Klason and acid-soluble lignin, an equal lignin composition, a similar amount and composition of hemicellulose, but a 3% increase in cellulose amount. Thus, the cell wall compositions of one-year-old *hpCAD* red and white patch wood were very alike, except for the increase in cellulose.

Third, the cell wall composition of three-year-old *hpCAD* poplars from H2 was determined (**Table 5, Table S3**). The %CWR expressed per dry weight was equal between three-year-old *hpCAD* lines and the WT, except for *hpCAD19*, which showed 1.3% less CWR. In contrast to one-year-old wood from H1, the Klason lignin amount and acid-insoluble lignin amount were not different between the three-year-old *hpCAD* and WT lines. On the other hand, similarly to one-year-old wood from H1, the cellulose amount was reduced by, on average, 3%, and the hemicellulose amount was increased by, on average, 4% in all three-year-old *hpCAD* lines when compared to the WT. Three-year-old *hpCAD* wood also showed shifts in the relative distribution of the main neutral sugars from the amorphous polysaccharides; when compared to the WT, all *hpCAD* lines consistently showed enrichments in Ara (of, on average, 17%) and Gal (of, on average, 18%) and a diminishment in Man (of, on average, 31%). Finally, the thioacidolysis-based determination of lignin composition showed that all *hpCAD* lignins released less monomers (H + G + S) when compared to WT lignins, indicative of a lower frequency of β-*O*-4 interunit bonds. The relative frequency of H units was increased by, on average, 79% in all *hpCAD* lines compared to the WT, while the S/G ratio and the relative frequency of G and S units in the *hpCAD* lines were equal to those of the WT. The abundance of coniferaldehyde-derived dithioketals in *hpCAD* lignins was not significantly different from that of WT lignin, while that of coniferaldehyde-derived indenes, sinapaldehyde-derived dithioketals and sinapaldehyde-derived indenes was increased by, on average, 11-, 3- and 128-fold, respectively in *hpCAD* lignins compared to WT lignins. In conclusion, clear differences existed in wood composition when one- and three-year-old *hpCAD* wood were compared. Perhaps most strikingly was the observation that three-year-old *hpCAD* wood was not different anymore in Klason lignin content and S/G ratio when compared to the WT.

Field-grown *hpCAD* wood displays improved saccharification after harsh alkaline pretreatments

Because lignin amount and composition greatly influence the hydrolysis of cell wall polysaccharides into primary sugars (i.e., saccharification), the saccharification potential of *hpCAD* wood was investigated under limited saccharification conditions. Saccharifications were preceded by no and (mild and harsh) alkaline pretreatments. The glucose release of one-year-old (from H1) and three-year-old (from H2) dried,

debarked wood was measured after 2, 6, 24 and 48 h of saccharification and normalized based on %CWR (**Fig. 3**).

The released glucose as %CWR of one-year-old *hpCAD* red wood from H1 was equal to that of the WT when no or mild alkaline (6.25 mM NaOH) pretreatments were applied (**Fig. 3a, b**). When a harsh (62.5 mM NaOH) alkaline pretreatment was applied and compared to the WT, the glucose release of one-year-old *hpCAD* red wood was increased with, on average, 85%, 79%, 74% and 60% after 2, 6, 24 and 48 h of saccharification, respectively (**Fig. 3c**).

When no or mild alkaline pretreatments were applied, the glucose release of one-year-old *hpCAD* white patch wood from H1 was increased compared to one-year-old *hpCAD* red wood from H1 with, on average, 31%, 37%, 43% and 60% (no pretreatment) and 72%, 82%, 85% and 66% (mild alkaline pretreatment) after 2, 6, 24 and 48 h of saccharification, respectively (**Fig. 3a, b**). When a harsh alkaline pretreatment was applied, one-year-old *hpCAD* white patch and red wood yielded similar amounts of glucose per CWR (**Fig. 3c**).

Because using mild alkaline pretreatments did not result in an increased saccharification efficiency in one-year-old *hpCAD* red wood from H1, only no and harsh alkaline pretreatments were applied on three-year-old *hpCAD* wood from H2. When no pretreatment was applied, the glucose release of three-year-old *hpCAD* wood from H2 was equal to that of the WT (**Fig. 3d**). When a harsh alkaline pretreatment was applied, the glucose release of three-year-old *hpCAD* wood was increased compared to the WT with, on average, 77%, 67%, 32% and 23% after 2, 6, 24 and 48 h of saccharification, respectively (**Fig. 3e**).

The glucose release after saccharification using harsh alkaline pretreatment was significantly higher in one- and three-year-old *hpCAD* wood compared to their WT control (**Fig. 3**). To take the yield penalty of one- and three-year-old *hpCAD* trees into account, their glucose yields were expressed on a plant basis (**Fig. S4**). After 48h of saccharification using harsh alkaline pretreatment and on a plant basis, one-year-old *hpCAD* trees had an, on average, 32% increase in sugar yield, while three-year-old *hpCAD* trees displayed an, on average, 42% reduction in sugar yield when compared to their WT control. These results show that the yield penalty observed in *hpCAD* trees partially (for one-year-old trees) or entirely (for three-year-old trees) off-sets the gains in fermentable sugar yield.

DISCUSSION

Lignin is one of the most important factors limiting the processing of plant biomass into fermentable sugars (Chen & Dixon, 2007; Studer *et al.*, 2011; Van Acker *et al.*, 2013; R. Vanholme *et al.*, 2013). When grown in the greenhouse, *hpCAD* poplar lines with severe reductions in CAD activity show normal growth and have enhanced amounts of cinnamaldehydes in the lignin and significant improvements in saccharification efficiency after alkaline pretreatment (Van Acker *et al.*, 2017). Here, these lines were grown in the field under SRC culture and evaluated for their biomass and wood properties and their interactions with the environment.

Field-grown *hpCAD* poplars show a significantly altered cell wall composition and increased saccharification efficiency

Similar to greenhouse-grown *hpCAD* poplars (Van Acker *et al.*, 2017), one-year-old field-grown *hpCAD* stems (from H1) had 10% less lignin when compared to the WT. By contrast, three-year-old field-grown *hpCAD* stems (from H2) had a lignin amount similar to that of the WT. Field trials with *4CL*- and *CCR*-downregulated poplars have also shown that the difference in lignin amount between transgenic and WT poplars was smaller (or even non-existent anymore) when the trees were grown in the field than when they were grown in the greenhouse (Stout *et al.*, 2014; Van Acker *et al.*, 2014; Xiang *et al.*, 2017). At least for CCR- and CAD-deficient poplars, it is possible that the smaller difference in lignin amount between transgenic and WT trees is due to the fact that the wood samples were taken during winter. When tree growth ceases in autumn, the trees still have time to further lignify their cell walls till they enter dormancy, whereas greenhouse-grown trees develop new xylem continuously. Alternatively, the relatively higher lignin content could have been a response to the environmental stress imposed to the yield-compromised 4CL-, CCR- and CAD-deficient trees. For example, CAD-deficient *Nicotiana attenuata* (tobacco) plants produce low-lignin, rubbery and structurally unstable stems when grown in the greenhouse (Kaur *et al.*, 2012). However, when planted into their native desert habitat, they produce robust stems that survive wind storms like WT plants do. Despite efficient silencing of *CAD* gene expression and reduced CAD enzymatic activity, field-grown CAD-deficient tobacco plants have total lignin contents that are comparable to the WT. When these CAD-deficient tobacco plants are grown in the field but protected from the environment, they again revert to a rubbery phenotype and reduced lignin contents similar to the

greenhouse-grown CAD-deficient plants (Kaur *et al.*, 2012). Another reason why three-year-old *hpCAD* poplars have the same lignin amount as WT poplars might be their reduced relative water content and free water available to support the hydraulic network (see further). Indeed, it has been shown that water deficit conditions may trigger an increase in lignin and hemicellulose levels in xylem cells walls (reviewed in Le Gall *et al.* (2015)). Finally, the observation that field-grown *hpCAD* poplars gradually fill up their cell wall with lignin might be due to a homeostasis mechanism and/or the action of the cell wall integrity monitoring pathway, as previously described (Bonawitz & Chapple, 2013; Muro-Villanueva *et al.*, 2019).

CAD-deficient dicot lignocellulosic biomass has been shown to have an increased susceptibility to alkaline degradation due to its altered lignin, including the enhanced incorporation of hydroxycinnamaldehydes (Baucher *et al.*, 1996; Ralph *et al.*, 2001; Lapierre *et al.*, 2004; Vanholme *et al.*, 2012; Anderson *et al.*, 2015; Carmona *et al.*, 2015; Van Acker *et al.*, 2017). The abundance of the latter was also significantly increased in lignin from greenhouse-grown *hpCAD* trees (Van Acker *et al.*, 2017) and in lignin of one- and three-year-old field-grown *hpCAD* trees analyzed here. Although greenhouse-grown and one-year-old field-grown *hpCAD* poplars had 10% less lignin, their saccharification efficiencies were only increased when an alkaline pretreatment preceded the saccharification protocol. A similar observation was made for CAD-deficient alfalfa that, despite having a reduced lignin amount, displayed no increase in saccharification yield after no or acid pretreatments (Jackson *et al.*, 2008). Another interesting observation was that greenhouse-grown *hpCAD* poplars show an increase in glucose release (as %CWR) after saccharification using mild alkaline and harsh alkaline pretreatments (Van Acker *et al.*, 2017), whereas field-grown *hpCAD* poplars only have an increase in glucose release (as %CWR) after saccharification using harsh alkaline pretreatments. These differences might be explained by the higher amount of (alkali-sensitive) hydroxycinnamaldehydes incorporated into the lignin of the greenhouse-grown *hpCAD* trees compared to the field-grown *hpCAD* trees: while coniferaldehyde- and sinapaldehyde-derived units constituted 7% of the thioacidolysis-released lignin monomers in greenhouse-grown *hpCAD* trees (Van Acker *et al.*, 2017), they only constituted 0.7% and 0.6% of the thioacidolysis-released lignin monomers in one-year-old and three-year-old field-grown *hpCAD* trees, respectively. The variability in the amount of cinnamaldehydes incorporated into the lignin polymer of greenhouse-grown and field-grown *hpCAD* poplars might be the consequence of differences in

gene silencing level, or in growth and development caused by the different environment.

The relative increase in glucose release (as %CWR) after saccharification using harsh alkaline pretreatment of field-grown *hpCAD* wood compared to WT wood decreased with increasing saccharification time; e.g., compared to their WT control, the 85% and 77% higher saccharification efficiency of one- and three-year-old *hpCAD* wood, respectively, after 2 h of saccharification using harsh alkaline pretreatment dropped to 60% and 23% after 48 h of saccharification. This indicates that *hpCAD* wood reached its saccharification plateau sooner and released its sugars faster during saccharification when compared to WT wood. Indeed, e.g. the glucose yield of one- and three-year-old WT wood after 24h of saccharification is comparable to that of one- and three-year-old *hpCAD* wood after only 6h of saccharification. These findings are important from an applied perspective, as less chemicals and/or time are needed to reach the same saccharification yield when *hpCAD* wood is used instead of WT wood.

Field-grown *hpCAD* trees display a leaning phenotype

When the *hpCAD* poplars are grown in the greenhouse, where they are supported and not exposed to leaning or bending loads caused by wind, rain or ice, they grow straight (Van Acker *et al.*, 2017). Nevertheless, greenhouse-grown *hpCAD* trees display a reduced wood stiffness that is, because of their unaltered wood density, solely attributed to the chemical differences at the cell wall level caused by *CAD1* downregulation (Özparpucu *et al.*, 2017). When *hpCAD* trees were grown in the field, they were leaning along with the prevailing wind direction. In contrast to greenhouse-grown *hpCAD* poplars (Özparpucu *et al.*, 2017), field-grown *hpCAD* poplars had a decreased wood density that, together with the changes in cell wall composition, most likely (further) decreased their wood stiffness, resulting in the observed leaning phenotype. Similarly, reduced stem stiffness was also observed in CAD-deficient Arabidopsis (based on the observed bending of the floral stems; Sibout *et al.*, 2005), tobacco (based on the determination of the tensile modulus; Hepworth & Vincent, 1998), and mulberry (based on the observed drooping branches; Yamamoto *et al.*, 2020).

One-year-old *hpCAD* white patch wood contained 3% more cellulose than one-year-old *hpCAD* red wood and displayed a white-colored zone in the middle of the otherwise dark-red-colored xylem. This white-colored zone probably contains tension

wood fibers that are typically induced upon leaning or bending stress (Clair *et al.*, 2011). Indeed, *ASCAD* poplars of which the stems had been exposed to bending loads formed tension wood that displayed a similar white-colored zone in the otherwise red-colored xylem (Pilate *et al.*, 2004). Tension wood fibers contain a thick extra cell wall layer (also called the G layer) that is very rich in cellulose with no or very low levels of lignin, making this cellulose very accessible even after no or very mild pretreatments (Brereton *et al.*, 2011). In line with this, the glucose release (as %CWR) after saccharification using no or mild pretreatments of one-year-old *hpCAD* white patch wood was increased when compared to that of one-year-old *hpCAD* red wood.

Severe downregulation of *CAD1* affects the biomass yield of field-grown poplars

In contrast to greenhouse-grown *hpCAD* trees (Van Acker *et al.*, 2017), field-grown *hpCAD* poplars displayed a strong yield penalty, already visible in one-year-old trees of the first growth cycle and even more pronounced in three-year-old trees of the second growth cycle. The biomass penalties of *hpCAD* trees were correlated with their reduced maximum growth rate, earlier growth cessation and earlier bud set.

Environmental factors such as temperature, wind and herbivory have already been shown to majorly impact the growth of lignin-engineered trees and CAD-deficient (tobacco and Medicago) plants (Voelker *et al.*, 2010; Kaur *et al.*, 2012; Zhao *et al.*, 2013; Van Acker *et al.*, 2014). Nevertheless, poplars with moderate reductions in CAD activity grow normally in the field (Lapierre *et al.*, 1999; Pilate *et al.*, 2002). Although the differences in growth in the field between poplars with moderate (*SCAD* and *ASCAD*) and severe (*hpCAD*) reductions in CAD activity might be the consequence of their different environment, it is more likely that the differences in biomass are the consequence of the more severe suppression of *CAD1* gene expression in the *hpCAD* poplars and the subsequent changes in metabolism and cell wall architecture.

The enlarged vessels, decreased wood density and reduced water content in field-grown *hpCAD* trees might be at the origin of the yield penalty

Various lignin-engineered plants, including CAD-deficient Arabidopsis and CCR-, C3'H-, and 4CL-deficient trees, displayed biomass yield penalties along with collapsed vessels (Leplé *et al.*, 2007; Coleman *et al.*, 2008; Wagner *et al.*, 2009; Voelker *et al.*, 2011; Sibout *et al*., 2015; De Meester *et al.*, 2020). The latter is probably the consequence of the reductions in lignin amount in these plants, weakening the vessel

cell wall resulting into vascular collapse under the negative pressure generated by transpiration (De Meester *et al.,* 2018). In contrast, three-year-old *hpCAD* poplars had WT lignin amounts and round, open and even enlarged vessels. These enlarged vessels might be caused by a longer vessel enlargement step [due to slower lignin deposition in the cell wall upon xylem maturation] or the significantly altered cell wall composition [including different cellulose/hemicellulose ratios and altered lignin and hemicellulose compositions] of field-grown *hpCAD* poplars. Interestingly, enlarged vessels have been observed before in growth-compromised greenhouse-grown CAD-deficient poplars (Miller *et al.,* 2019).

Larger vessels generally lead to enhanced sensitivity to embolism (Wheeler *et al.*, 2005). Next to larger vessels, also the decreased wood density of *hpCAD* poplars could contribute to enhanced xylem vulnerability to embolism (Awad *et al.*, 2012), meaning that *hpCAD* poplars are more likely to experience disruptions of sap transport in xylem conduits and water supply to the leaves. Poplars are already among the tree species that are most sensitive to xylem embolism and the resistance to xylem embolism has been shown to be even lower in several transgenic, lignin-engineered poplar lines when compared to WT trees (Sperry *et al.*, 1991; Cochard *et al.*, 2007; Coleman *et al.*, 2008; Fichot *et al.*, 2010; Voelker *et al.*, 2011). For example, greenhouse-grown poplars downregulated in *C3'H, CCR, COMT* or *CAD* and field-grown poplars downregulated in *4CL* are more sensitive to embolism, although in these cases this was not associated with enlarged vessels (but rather collapsed vessels for *CCR*, *C3'H*- and *4CL*-downregulated poplars and normal vessels for *CAD*- and *COMT*-downregulated poplars) (Coleman *et al.*, 2008; Voelker *et al.*, 2011; Awad *et al.*, 2012). Although only greenhouse-grown *C3'H*- and field-grown *4CL*-downregulated poplars display yield penalties (while *CCR*-, *COMT*- and *CAD*-downregulated poplars grew normally in the greenhouse), the susceptibility to embolism might be very important for plant growth, especially in the field where the plants are exposed to different kinds of stresses (e.g. drought). Indeed, as said above, *CCR*-downregulated poplars grew normally in the greenhouse (despite their enhanced susceptibility to embolism (Awad *et al.*, 2012)), but displayed a yield penalty when grown in the field (Leplé *et al.*, 2007). Next to sensitivity to embolism, also water availability influences the growth of lignin mutants (Marchin *et al.*, 2017). Here, we found that field-grown *hpCAD* wood had a reduced relative water content when compared to the WT. This feature was further enhanced by the relatively higher amount of water bound to the xylem cell wall (α_f) of

hpCAD wood. As this bound water is inaccessible to plants for transport, *hpCAD* wood had a reduced amount of free water available to support the hydraulic network when compared to the WT. Hypothetically, the proposed enhanced sensitivity to embolism and the reduced water availability could make *hpCAD* poplars less resistant to drought stress (Awad *et al.*, 2012), which might be associated with their premature growth arrest/bud set and yield penalty. Interestingly, silencing of *CAD2* or *CAD3* in melon also resulted in dwarfed phenotypes, lower relative water contents and reduced drought tolerance (Liu *et al*., 2020).

Severe downregulation of *CAD1* affects the timing of flowering but has no major impact on the susceptibility to pathogens of field-grown trees

In addition to early bud set in fall, field-grown *hpCAD* poplars also displayed early flowering in spring. As far as we know, early flowering has not been observed before in field-grown lignin-engineered trees and is of great relevance concerning biosafety aspects of field trials. Indeed, because *P. tremula* x *P. alba* normally only develops flowers after five to eight years, SRC culture *P. tremula* x *P. alba* trees are not expected to flower because the stems are harvested every three years. Nevertheless, in our field-trial, two- and three-year-old trees of the second growth cycle developed flowers. Although this might suggest that CAD1 has a dual role in poplar, being involved in lignin biosynthesis and flowering, it is far more likely that the early flowering observed here is the consequence of water deficits experienced by the *hpCAD* lines due to the altered water availability. Indeed, it has been shown that water deficit conditions induce flowering in trees (Southwick & Davenport, 1986; Takeno, 2016; Wu *et al.*, 2017). Because in 2016-2017 a record-breaking drought took place in Europe (García-Herrera *et al.*, 2019), it is not surprising that we observed early flowering in two- and three-year-old *hpCAD* lines (which might be less tolerant to drought stress as discussed above) and even that a few flowers emerged on a three-year-old WT tree.
Despite the severe yield penalty and significant developmental and cell wall changes of *hpCAD* poplars, and in line with the earlier observations on field-grown, less severely *CAD*-downregulated poplars (Pilate *et al.*, 2002; Halpin *et al.*, 2007), no major changes in susceptibility to pests and diseases were found (**Table 1, Table 4, Table 5**).

Conclusion

In strong contrast to greenhouse-grown *hpCAD* trees and previous field trials with poplars less severely downregulated for *CAD*, we found that field-grown *hpCAD* poplars displayed undesirable phenotypes such as growth perturbations, leaning phenotypes, early bud set and early flowering. In contrast to greenhouse-grown and one-year-old field grown *hpCAD* trees, three-year-old *hpCAD* poplars had WT lignin levels but, because of their significantly altered cell wall composition, still exhibited an enhanced glucose release (as %CWR) after saccharification using alkaline pretreatment. However, the gains in fermentable sugar yield after saccharification using alkaline pretreatment were partially (for one-year-old *hpCAD* trees) or entirely (for three-year-old *hpCAD* trees) off-set by their yield penalty. Interestingly, despite their significantly altered phenotypes and lignin, *hpCAD* poplars showed no major differences in susceptibility to pathogens and insects. Our results show the importance of multi-year field trials early in scientific development.

ACKNOWLEDGEMENTS

We thank Annick Bleys for help in preparing the article, Kurt Schamp for helping in determining the insect and rust tolerance and Sandrien Desmet of the VIB Metabolomics Core Ghent for analysis of the thioacidolysis GC-MS chromatograms. B.D.M. is indebted to the Research Foundation Flanders (FWO) for a postdoctoral fellowship, M.W. was funded by FWO for a predoctoral fellowship, S.T. was funded by the Agrobiosciences PhD program at Scuola Superiore Sant'Anna of Pisa. W.B. acknowledges funding from the SBO project Bioleum, the Energy Transition Fund (ETF) projects ADV_BIO and AD-LIBIO, and from the EU-funded projects Energypoplar, Renewall and MultiBioPro.

AUTHOR CONTRIBUTIONS

BDM, RVA, and WB designed the research; BDM, RVA, MW, ST, MS and JN performed the experiments; BDM, RVA, MW, ST and FVB performed the data analysis; BDM wrote the article with contributions from all authors.

DATA AVAILABILITY

Data supporting the findings of this work are available within the paper and its Supplementary Information files.

REFERENCES

Anderson NA, Tobimatsu Y, Ciesielski PN, Ximenes E, Ralph J, Donohoe BS, Ladisch M, Chapple C. 2015. Manipulation of guaiacyl and syringyl monomer biosynthesis in an Arabidopsis cinnamyl alcohol dehydrogenase mutant results in atypical lignin biosynthesis and modified cell wall structure. *Plant Cell* **27:** 2195-2209.

Awad H, Herbette S, Brunel N, Tixier A, Pilate G, Cochard H, Badel E. 2012. No trade-off between hydraulic and mechanical properties in several transgenic poplars modified for lignins metabolism. *Environmental and Experimental Botany* **77:** 185-195.

Baucher M, Chabbert B, Pilate G, Van Doorsselaere J, Tollier MT, Petit-Conil M, Cornu D, Monties B, Van Montagu M, Inzé D*, et al.* 1996. Red xylem and higher lignin extractability by down-regulating a cinnamyl alcohol dehydrogenase in poplar. *Plant Physiology* **112:** 1479-1490.

Bonawitz ND, Chapple C. 2013. Can genetic engineering of lignin deposition be accomplished without an unacceptable yield penalty? *Current Opinion in Biotechnology* **24:** 336-343.

Brendel O, Iannetta PPM, Stewart D. 2000. A rapid and simple method to isolate pure alpha-cellulose. *Phytochemical Analysis* **11:** 7-10.

Brereton NJB, Pitre FE, Ray MJ, Karp A, Murphy RJ. 2011. Investigation of tension wood formation and 2,6-dichlorbenzonitrile application in short rotation coppice willow composition and enzymatic saccharification. *Biotechnology for Biofuels* **4:** 13.

Carmona C, Langan P, Smith JC, Petridis L. 2015. Why genetic modification of lignin leads to low-recalcitrance biomass. *Physical Chemistry Chemical Physics* **17:** 358-364.

Chanoca A, de Vries L, Boerjan W. 2019. Lignin engineering in forest trees. *Frontiers in Plant Science* **10:** 912.

Chen F, Dixon RA. 2007. Lignin modification improves fermentable sugar yields for biofuel production. *Nature Biotechnology* **25:** 759-761.

Clair B, Alméras T, Pilate G, Jullien D, Sugiyama J, Riekel C. 2011. Maturation stress generation in poplar tension wood studied by synchrotron radiation microdiffraction. *Plant Physiology* **155:** 562-570.

Cochard H, Casella E, Mencuccini M. 2007. Xylem vulnerability to cavitation varies among poplar and willow clones and correlates with yield. *Tree Physiology* **27:** 1761-1767.

Coleman HD, Samuels AL, Guy RD, Mansfield SD. 2008. Perturbed lignification impacts tree growth in hybrid poplar - A function of sink strength, vascular integrity, and photosynthetic assimilation. *Plant Physiology* **148:** 1229-1237.

De Meester B, de Vries L, Ozparpucu M, Gierlinger N, Corneillie S, Pallidis A, Goeminne G, Morreel K, De Bruyne M, De Rycke R*, et al.* 2018. Vessel-Specific Reintroduction of CINNAMOYL-COA REDUCTASE1 (CCR1) in Dwarfed ccr1 Mutants Restores Vessel and Xylary Fiber Integrity and Increases Biomass. *Plant Physiol* **176:** 611-633.

De Meester B, Madariaga Calderón B, de Vries L, Pollier J, Goeminne G, Van Doorsselaere J, Chen M, Ralph J, Vanholme R, Boerjan W. 2020. Tailoring poplar lignin without yield penalty by combining a null and haploinsufficient *CINNAMOYL-CoA REDUCTASE2* allele. *Nature Communications* **11:** 5020.

Eudes A, George A, Mukerjee P, Kim JS, Pollet B, Benke PI, Yang F, Mitra P, Sun L, Çetinkol ÖP*, et al.* 2012. Biosynthesis and incorporation of side-chain-truncated lignin monomers to reduce lignin polymerization and enhance saccharification. *Plant Biotechnology Journal* **10:** 609-620.

Fetting C. 2020. The European Green Deal. *ESDN Report, December 2020, ESDN Office, Vienna*.

Fichot R, Barigah TS, Chamaillard S, Le Thiec D, Laurans F, Cochard H, Brignolas F. 2010. Common trade-offs between xylem resistance to cavitation and other physiological traits do not hold among unrelated *Populus deltoidesx Populus nigra* hybrids. *Plant Cell and Environment* **33:** 1553-1568.

Foster C, Martin T, Pauly M. 2010. Comprehensive compositional analysis of plant cell walls (lignocellulosic biomass). Part II: Carbohydrates. *Journal of Visualized Experiments* **37:** 1837.

Freudenberg K. 1959. Biosynthesis and constitution of lignin. *Nature* **183:** 1152-1155.

Gao D, Haarmeyer C, Balan V, Whitehead TA, Dale BE, Chundawat SPS. 2014. Lignin triggers irreversible cellulase loss during pretreated lignocellulosic biomass saccharification. *Biotechnology for Biofuels* **7:** 175.

García-Herrera R, Garrido-Perez JM, Barriopedro D, Ordóñez C, Vicente-Serrano SM, Nieto R, Gimeno L, Sori R, Yiou P. 2019. The European 2016/17 drought. *Journal of Climate* **32:** 3169-3187.

Halpin C, Thain SC, Tilston EL, Guiney E, Lapierre C, Hopkins DW. 2007. Ecological impacts of trees with modified lignin. *Tree Genetics & Genomes* **3:** 101-110.

Hepworth DG, Vincent JFV. 1998. Modelling the mechanical properties of xylem tissue from tobacco plants (*Nicotiana tabacum* 'Samsun') by considering the importance of molecular and micromechanisms. *Annals of Botany* **81:** 761-770.

Ibáñez AB, Bauer S. 2014. Downscaled method using glass microfiber filters for the determination of Klason lignin and structural carbohydrates. *Biomass & Bioenergy* **68:** 75-81.

Jackson LA, Shadle GL, Zhou R, Nakashima J, Chen F, Dixon RA. 2008. Improving saccharification efficiency of alfalfa stems through modification of the terminal stages of monolignol biosynthesis. *BioEnergy Research* **1:** 180-192.

Kaur H, Shaker K, Heinzel N, Ralph J, Gális I, Baldwin IT. 2012. Environmental stresses of field growth allow cinnamyl alcohol dehydrogenase-deficient *Nicotiana attenuata* plants to compensate for their structural deficiencies. *Plant Physiology* **159:** 1545-1570.

Lapierre C, Pilate G, Pollet B, Mila I, Leplé J-C, Jouanin L, Kim H, Ralph J. 2004. Signatures of cinnamyl alcohol dehydrogenase deficiency in poplar lignins. *Phytochemistry* **65:** 313-321.

Lapierre C, Pollet B, Petit-Conil M, Toval G, Romero J, Pilate G, Leplé J-C, Boerjan W, Ferret V, De Nadai V*, et al.* 1999. Structural alterations of lignins in transgenic poplars with depressed cinnamyl alcohol dehydrogenase or caffeic acid*O*-methyltransferase activity have an opposite impact on the efficiency of industrial kraft pulping. *Plant Physiology* **119:** 153-164.

Le Gall H, Philippe F, Domon J-M, Gillet F, Pelloux J, Rayon C. 2015. Cell wall metabolism in response to abiotic stress. *Plants* **4:** 112-166.

Leplé J-C, Dauwe R, Morreel K, Storme V, Lapierre C, Pollet B, Naumann A, Kang K-Y, Kim H, Ruel K*, et al.* 2007. Downregulation of cinnamoyl-coenzyme A reductase in poplar: multiple-level phenotyping reveals effects on cell wall polymer metabolism and structure. *Plant Cell* **19:** 3669-3691.

Liu W, Jiang Y, Wang C, Zhao L, Jin Y, Xing Q, Li M, Lv T, Qi H. 2020. Lignin synthesized by CmCAD2 and CmCAD3 in oriental melon (Cucumis melo L.) seedlings contributes to drought tolerance. *Plant Mol Biol* **103:** 689-704.

Marchin RM, Stout AT, Davis AA, King JS. 2017. Transgenically altered lignin biosynthesis affects photosynthesis and water relations of field-grown *Populus trichocarpa*. *Biomass & Bioenergy* **98:** 15-25.

Marriott PE, Gómez LD, McQueen-Mason SJ. 2016. Unlocking the potential of lignocellulosic biomass through plant science. *New Phytologist* **209:** 1366-1381.

Miller ZD, Peralta PN, Mitchell P, Chiang VL, Kelley SS, Edmunds CW, Peszlen IM. 2019. Anatomy and Chemistry of Populus trichocarpa with Genetically Modified Lignin Content. *BioResources* **14**.

Mottiar Y, Vanholme R, Boerjan W, Ralph J, Mansfield SD. 2016. Designer lignins: harnessing the plasticity of lignification. *Current Opinion in Biotechnology* **37:** 190-200.

Muro-Villanueva F, Mao X, Chapple C. 2019. Linking phenylpropanoid metabolism, lignin deposition, and plant growth inhibition. *Current Opinion in Biotechnology* **56:** 202-208.

Oyarce P, De Meester B, Fonseca F, de Vries L, Goeminne G, Pallidis A, De Rycke R, Tsuji Y, Li Y, Van den Bosch S*, et al.* 2019. Introducing curcumin biosynthesis in *Arabidopsis* enhances lignocellulosic biomass processing. *Nature Plants* **5:** 225-237.

Özparpucu M, Rüggeberg M, Gierlinger N, Cesarino I, Vanholme R, Boerjan W, Burgert I. 2017. Unravelling the impact of lignin on cell wall mechanics: a comprehensive study on young poplar trees downregulated for CINNAMYL ALCOHOL DEHYDROGENASE (CAD). *Plant Journal* **91:** 480-490.

Perkins M, Smith RA, Samuels L. 2019. The transport of monomers during lignification in plants: anything goes but how? *Current Opinion in Biotechnology* **56:** 69-74.

Pilate G, Allona I, Boerjan W, Déjardin A, Fladung M, Gallardo Alba F, Häggman H, Jansson S, Van Acker R, Halpin C. 2015. Field trials with genetically engineered forest trees: past experiences and future prospects. *IUFRO Tree Biotechnology Conference 2015; Treebiotech2015, IUFRO., Jun 2015, Florence, Italy (https://hal.inrae.fr/hal-02741586)*.

Pilate G, Chabbert B, Cathala B, Yoshinaga A, Leplé J-C, Laurans F, Lapierre C, Ruel K. 2004. Lignification and tension wood. *Comptes Rendus Biologies* **327:** 889-901.

Pilate G, Guiney E, Holt K, Petit-Conil M, Lapierre C, Leplé J-C, Pollet B, Mila I, Webster EA, Marstorp HG*, et al.* 2002. Field and pulping performances of transgenic trees with altered lignification. *Nature Biotechnology* **20:** 607-612.

Ralph J, Lapierre C, Boerjan W. 2019. Lignin structure and its engineering. *Current Opinion in Biotechnology* **56:** 240-249.

Ralph J, Lapierre C, Marita JM, Kim H, Lu F, Hatfield RD, Ralph S, Chapple C, Franke R, Hemm MR*, et al.* 2001. Elucidation of new structures in lignins of CAD- and COMT-deficient plants by NMR. *Phytochemistry* **57:** 993-1003.

Rinaldi R, Jastrzebski R, Clough MT, Ralph J, Kennema M, Bruijnincx PCA, Weckhuysen BM. 2016. Paving the way for lignin valorisation: Recent advances in bioengineering, biorefining and catalysis. *Angewandte Chemie. International Edition* **55:** 8164-8215.

Robinson AR, Mansfield SD. 2009. Rapid analysis of poplar lignin monomer composition by a streamlined thioacidolysis procedure and near-infrared reflectance-based prediction modeling. *Plant Journal* **58:** 706-714.

Santiago LS, Goldstein G, Meinzer FC, Fisher JB, Machado K, Woodruff D, Jones T. 2004. Leaf photosynthetic traits scale with hydraulic conductivity and wood density in Panamanian forest canopy trees. *Oecologia* **140:** 543-550.

Schneider CA, Rasband WS, Eliceiri KW. 2012. NIH Image to ImageJ: 25 years of image analysis. *Nature Methods* **9:** 671-675.

Schutyser W, Renders T, Van den Bosch S, Koelewijn S-F, Beckham GT, Sels BF. 2018. Chemicals from lignin: an interplay of lignocellulose fractionation, depolymerisation, and upgrading. *Chemical Society Reviews* **47:** 852-908.

Sibout R, Eudes A, Mouille G, Pollet B, Lapierre C, Jouanin L, Séguin A. 2005. *CINNAMYL ALCOHOL DEHYDROGENASE-C* and *-D* are the primary genes involved in lignin biosynthesis in the floral stem of Arabidopsis. *Plant Cell* **17:** 2059-2076.

Sibout R, Le Bris P, Legée F, Cézard L, Renault H, Lapierre C. 2016. Structural redesigning arabidopsis lignins into alkali-soluble lignins through the expression of *p*-coumaroyl-CoA:monolignol transferase PMT. *Plant Physiology* **170:** 1358-1366.

Singh N, Singhania RR, Nigam PS, Dong C-D, Patel AK, Puri M. 2022. Global status of lignocellulosic biorefinery: challenges and perspectives. *Bioresource Technology* **344:** 126415.

Smith RA, Gonzales-Vigil E, Karlen SD, Park J-Y, Lu F, Wilkerson CG, Samuels L, Ralph J, Mansfield SD. 2015. Engineering monolignol *p*-coumarate conjugates into poplar and Arabidopsis lignins. *Plant Physiology* **169:** 2992-3001.

Southwick SM, Davenport TL. 1986. Characterization of water stress and low temperature effects on flower induction in citrus. *Plant Physiology* **81:** 26-29.

Sperry JS, Perry AH, Sullivan JEM. 1991. Pit membrane degradation and air-embolism formation in aging xylem vessels of *Populus tremuloides* Michx. *Journal of Experimental Botany* **42:** 1399-1406.

Sperry JS, Saliendra NZ. 1994. Intra-plant and inter-plant variation in xylem cavitation in *Betula occidentalis*. *Plant Cell and Environment* **17:** 1233-1241.

Stout AT, Davis AA, Domec J-C, Yang CM, Shi R, King JS. 2014. Growth under field conditions affects lignin content and productivity in transgenic *Populus trichocarpa* with altered lignin biosynthesis. *Biomass & Bioenergy* **68:** 228-239.

Studer MH, DeMartini JD, Davis MF, Sykes RW, Davison B, Keller M, Tuskan GA, Wyman CE. 2011. Lignin content in natural Populus variants affects sugar release. *Proceedings of the National Academy of Sciences of the United States of America* **108:** 6300-6305.

Takeno K. 2016. Stress-induced flowering: the third category of flowering response. *Journal of Experimental Botany* **67:** 4925-4934.

Traversari S, Francini A, Traversi ML, Emiliani G, Sorce C, Sebastiani L, Giovannelli A. 2018. Can sugar metabolism in the cambial region explain the water deficit tolerance in poplar? *Journal of Experimental Botany* **69:** 4083-4097.

Van Acker R, Déjardin A, Desmet S, Hoengenaert L, Vanholme R, Morreel K, Laurans F, Kim H, Santoro N, Foster C*, et al.* 2017. Different routes for conifer- and sinapaldehyde and higher saccharification upon deficiency in the dehydrogenase CAD1. *Plant Physiology* **175:** 1018-1039.

Van Acker R, Leplé J-C, Aerts D, Storme V, Goeminne G, Ivens B, Légée F, Lapierre C, Piens K, Van Montagu MCE*, et al.* 2014. Improved saccharification and ethanol yield from field-grown transgenic poplar deficient in cinnamoyl-CoA reductase. *Proceedings of the National Academy of Sciences of the United States of America* **111:** 845-850.

Van Acker R, Vanholme R, Piens K, Boerjan W. 2016. Saccharification protocol for small-scale lignocellulosic biomass samples to test processing of cellulose into glucose. *Bio-Protocol* **6:** e1701 (http://www.bio-protocol.org/e1701).

Van Acker R, Vanholme R, Storme V, Mortimer JC, Dupree P, Boerjan W. 2013. Lignin biosynthesis perturbations affect secondary cell wall composition and saccharification yield in *Arabidopsis thaliana*. *Biotechnology for Biofuels* **6:** 46.

Vanholme B, Desmet T, Ronsse F, Rabaey K, Van Breusegem F, De Mey M, Soetaert W, Boerjan W. 2013. Towards a carbon-negative sustainable bio-based economy. *Frontiers in Plant Science* **4:** 174.

Vanholme R, Cesarino I, Rataj K, Xiao Y, Sundin L, Goeminne G, Kim H, Cross J, Morreel K, Araujo P*, et al.* 2013. Caffeoyl shikimate esterase (CSE) is an enzyme in the lignin biosynthetic pathway in *Arabidopsis*. *Science* **341:** 1103-1106.

Vanholme R, De Meester B, Ralph J, Boerjan W. 2019. Lignin biosynthesis and its integration into metabolism. *Current Opinion in Biotechnology* **56:** 230-239.

Vanholme R, Morreel K, Darrah C, Oyarce P, Grabber JH, Ralph J, Boerjan W. 2012. Metabolic engineering of novel lignin in biomass crops. *New Phytologist* **196:** 978-1000.

Vermaas JV, Dixon RA, Chen F, Mansfield SD, Boerjan W, Ralph J, Crowley MF, Beckham GT. 2019. Passive membrane transport of lignin-related compounds. *Proceedings of the National Academy of Sciences of the United States of America* **116:** 23117-23123.

Voelker SL, Lachenbruch B, Meinzer FC, Jourdes M, Ki C, Patten AM, Davin LB, Lewis NG, Tuskan GA, Gunter L*, et al.* 2010. Antisense down-regulation of *4CL* expression alters lignification, tree growth, and saccharification potential of field-grown poplar. *Plant Physiology* **154:** 874-886.

Voelker SL, Lachenbruch B, Meinzer FC, Kitin P, Strauss SH. 2011. Transgenic poplars with reduced lignin show impaired xylem conductivity, growth efficiency and survival. *Plant Cell and Environment* **34:** 655-668.

Voorend W, Lootens P, Nelissen H, Roldán-Ruiz I, Inzé D, Muylle H. 2014. LEAF-E: a tool to analyze grass leaf growth using function fitting. *Plant Methods* **10:** 37.

Wagner A, Donaldson L, Kim H, Phillips L, Flint H, Steward D, Torr K, Koch G, Schmitt U, Ralph J. 2009. Suppression of 4-coumarate-CoA ligase in the coniferous gymnosperm *Pinus radiata*. *Plant Physiology* **149:** 370-383.

Wheeler JK, Sperry JS, Hacke UG, Hoang N. 2005. Inter-vessel pitting and cavitation in woody Rosaceae and other vesselled plants: a basis for a safety versus efficiency trade-off in xylem transport. *Plant Cell and Environment* **28:** 800-812.

Wilkerson CG, Mansfield SD, Lu F, Withers S, Park J-Y, Karlen SD, Gonzales-Vigil E, Padmakshan D, Unda F, Rencoret J*, et al.* 2014. Monolignol ferulate

transferase introduces chemically labile linkages into the lignin backbone. *Science* **344:** 90-93.

Wu P, Wu C, Zhou B. 2017. Drought stress induces flowering and enhances carbohydrate accumulation in *Averrhoa Carambola*. *Horticultural Plant Journal* **3:** 60-66.

Xiang Z, Sen SK, Min D, Savithri D, Lu F, Jameel H, Chiang V, Chang H-m. 2017. Field-grown transgenic hybrid poplar with modified lignin biosynthesis to improve enzymatic saccharification efficiency. *ACS Sustainable Chemistry & Engineering* **5:** 2407-2414.

Yamamoto M, Tomiyama H, Koyama A, Okuizumi H, Liu S, Vanholme R, Goeminne G, Hirai Y, Shi H, Nuoendagula*, et al.* 2020. A century-old mystery unveiled: Sekizaisou is a natural lignin mutant. *Plant Physiology* **182:** 1821-1828.

Zhao Q, Tobimatsu Y, Zhou R, Pattathil S, Gallego-Giraldo L, Fu C, Jackson LA, Hahn MG, Kim H, Chen F*, et al.* 2013. Loss of function of cinnamyl alcohol dehydrogenase 1 leads to unconventional lignin and a temperature-sensitive growth defect in *Medicago truncatula*. *Proceedings of the National Academy of Sciences of the United States of America* **110:** 13660-13665.

SUPPORTING INFORMATION

Additional Supporting Information may be found online in the Supporting Information for this article:

Fig. S1. Field trial set-up and short rotation coppice (SRC) scheme.

Fig. S2. Bud set and flowering in field-grown *hpCAD* poplars.

Fig. S3. Wood anatomy of field-grown *hpCAD* poplars.

Fig. S4. Glucose yield per tree after saccharification of field-grown *hpCAD* poplars.

Table S1. Summary of specific quantifier, qualifiers and retention time (RT) used for GC-MS-based analysis of lignin monomers of CWR of H1 released upon thioacidolysis.

Table S2. Method and summary of specific quantifier, qualifiers and retention time (RT) used for GC-MS-based analysis of lignin monomers of CWR of H2 released upon thioacidolysis.

Table S3. Absolute values for H/G/S lignin composition determined via thioacidolysis of field-grown *hpCAD* and WT poplars.

Note S1. Detailed information on the two growth cycles, phenotyping and harvests of *hpCAD* poplars grown in the field.

TABLES

Table 1. Biomass characteristics of field-grown *hpCAD* and WT poplars.

	Growth and harvest 1				Growth and harvest 2											
	2014 (harvest Feb. 2015 – H1)				2015				2016				2017 (harvest Mar. 2018 – H2)			
	WT	*hpCAD4*	*hpCAD19*	*hpCAD24*	WT	*hpCAD4*	*hpCAD19*	*hpCAD24*	WT	*hpCAD4*	*hpCAD19*	*hpCAD24*	WT	*hpCAD4*	*hpCAD19*	*hpCAD24*
Maximal growth rate (cm/day)[a]	2.5 ± 0.3	2.2 ± 0.2	2.4 ± 0.4	2.3 ± 0.3	3.0 ± 0.2	2.8 ± 0.2	2.8 ± 0.2	2.8 ± 0.2	n.d.				n.d.			
Growth arrest (days after planting in the field (2014) or after bud flush (2015))[a]	240 ± 5	231 ± 9	221 ± 22	236 ± 7	221 ± 4	211 ± 5	216 ± 4	216 ± 4	n.d.				n.d.			
Height (cm)[a]	296 ± 34	264 ± 31	267 ± 39	273 ± 40	377 ± 28	328 ± 18	342 ± 24	345 ± 24	n.d.				693 ± 60	419 ± 47	445 ± 54	455 ± 57
Number of stems[a]	n.a.				3.4 ± 1.1	3.5 ± 0.9	3.3 ± 0.9	3.3 ± 0.9	4.4 ± 1.2	**4.8 ± 1.2**	4.4 ± 1.1	4.3 ± 1.2	6.4 ± 1.6	6.2 ± 1.5	5.7 ± 1.3	5.7 ± 1.6
Diameter main stem (mm)[a]	21.9 ± 2.4	20.5 ± 1.7	20.0 ± 2.5	20.4 ± 2.3	24.1 ± 3.9	18.8 ± 2.5	20.6 ± 2.2	21.1 ± 2.1	38.0 ± 5.4	26.7 ± 3.5	27.7 ± 4.0	29.3 ± 4.3	45.8 ± 10.4	31.7 ± 6.5	33.2 ± 7.6	35.0 ± 8.3
Diameter 2nd stem (cm)[a]	n.a.				n.d.				n.d.				20.3 ± 7.0	**25.3 ± 6.2**	**26.9 ± 6.6**	**27.9 ± 7.5**
Diameter 3rd stem (cm)[a]	n.a.				n.d.				n.d.				13.2 ± 3.8	**19.8 ± 5.7**	**18.3 ± 6.3**	**18.8 ± 6.3**
Weight bottom 1 m (g)[b]	181 ± 38	146 ± 24 (143 ± 32)[$]	150 ± 44 (157 ± 40)[$]	154 ± 27 (134 ± 33)[$]	n.a.				n.a.				872 ± 283	326 ± 88	456 ± 109	463 ± 169
Weight total tree (kg)[a]	0.45 ± 0.09	0.34 ± 0.05	0.35 ± 0.10	0.36 ± 0.05	n.a.				n.a.				8.5 ± 2.8	5.1 ± 1.4	6.3 ± 1.3	5.8 ± 1.6

The height was measured on a monthly basis during the growth season of 2014 and 2015. Based on these monthly measurements, the maximum growth rate and the timing of the growth arrest (in autumn) was determined using LEAF-E. The final height was measured in the winter at the end of the year 2014, 2015 and 2017. In 2014, all trees grew as a single stem, whereas after coppicing/harvesting, multiple stems sprouted from the stools. The total number of stems was counted in winter of the end of the year 2015, 2016 and 2017. In addition, in 2017, also the diameter of the second and third thickest stem was measured for each tree. The dry weight of the bottom 1 meter of the harvested stem of H1 is shown separately for red *hpCAD* trees (upper value) and white patch *hpCAD* trees (lower value indicated between brackets). Total tree weight was calculated based on the dry weights of the chopped wood per block and per line (see Note S1). The data represent means ± SD. Values in bold font or underlined values indicate significantly increased or decreased values, respectively, as compared to those of the WT or [$]in case of white patch *hpCAD* wood from H1, as compared to those of red *hpCAD* wood of H1 (Two-way ANOVA with Dunnett's post-hoc test; $P < 0.05$; [a]n = 240 biologically independent samples; [b]n = 54 biologically independent samples for WT and red *hpCAD* trees of H1, n = 19 biologically independent *hpCAD4* samples for white patch trees of H1, n = 6 biologically independent *hpCAD19* samples for white patch trees of H1, n = 10 biologically independent *hpCAD24* samples for white patch trees of H1, n = 18 biologically independent samples for H2). n.d.: not determined; n.a., not applicable.

Table 2. Anatomical analyses of stem cross sections of field-grown *hpCAD* and WT poplars.

Parameter	Line			
	WT	*hpCAD4*	*hpCAD19*	*hpCAD24*
D_H (µm)	48.3 ± 1.8	**55.1 ± 3.7**	**54.5 ± 3.4**	**54.1 ± 3.7**
Vessel area (mm^2)	0.12 ± 0.01	**0.18 ± 0.02**	**0.16 ± 0.02**	**0.16 ± 0.03**
$K_{(S)t}$ ($kg\ s^{-1}m^{-1}\ MPa^{-1}$)	8.0 ± 1.3	**15.7 ± 3.9**	**13.7 ± 3.7**	**13.6 ± 3.4**

D_H, hydraulically weighted vessel diameter; $K_{S(t)}$, theoretical specific xylem hydraulic conductivity. The data represent means ± SD. Values in bold font indicate significantly increased values as compared to those of the WT (Two-way ANOVA with Dunnett's post-hoc test; $P < 0.05$; n = 6 biologically independent samples per line from H2).

Table 3. Relative water content (RWC) and wood traits of field-grown *hpCAD* and WT poplars.

Parameter	Line			
	WT	*hpCAD4*	*hpCAD19*	*hpCAD24*
Bark RWC (%)	83.2 ± 4.2	80.7 ± 3.7	80.9 ± 3.4	82.8 ± 6.7
Wood RWC (%)	71.7 ± 5.1	42.0 ± 6.6	51.2 ± 6.8	48.5 ± 14.1
α_f	0.35 ± 0.01	**0.38 ± 0.01**	**0.38 ± 0.00**	**0.37 ± 0.01**
α-α_f	0.88 ± 0.12	0.51 ± 0.12	0.68 ± 0.15	0.59 ± 0.28
Basic density (kg m^{-3})	405.8 ± 20.3	332.8 ± 21.0	333.7 ± 7.6	345.1 ± 23.0

The data represent means ± SD. α_f, fibre saturation point; α-α_f, free water available to support the hydraulic network. Values in bold font or underlined values indicate significantly increased or decreased values, respectively, as compared to those of the WT (Two-way ANOVA with Dunnett's post-hoc test; $P < 0.05$; n = 6 biologically independent samples per line from H2).

Table 4. Biological interactions of field-grown *hpCAD* and WT poplars.

			Rust infection		Insect damage	
Harvest	Year	Line	Incidence score (n)	Severity score (n)	Incidence score (n)	Severity score (n)
H1	2014	WT	0.89 ± 0.32 (96)	4.02 ± 0.63 (96)	n.d.	n.d.
		hpCAD4	0.84 ± 0.26 (96)	3.92 ± 0.45 (96)		
		hpCAD19	0.94 ± 0.35 (96)	4.05 ± 0.44 (96)		
		hpCAD24	0.84 ± 0.37 (96)	3.96 ± 0.56 (96)		
H2	2015	WT	1.49 ± 0.26 (160)	4.62 ± 0.56 (160)	1.42 ± 0.50 (160)	4.02 ± 0.58 (160)
		hpCAD4	1.41 ± 0.25 (160)	4.39 ± 0.49 (160)	1.41 ± 0.49 (160)	3.96 ± 0.56 (160)
		hpCAD19	1.45 ± 0.27 (160)	4.36 ± 0.48 (160)	**1.56 ± 0.55 (160)**	4.06 ± 0.60 (160)
		hpCAD24	1.54 ± 0.18 (160)	4.43 ± 0.51 (160)	1.38 ± 0.49 (160)	3.95 ± 0.51 (160)
	2017	WT	2.51 ± 0.58 (120)	n.d.	1.89 ± 0.32 (90)	n.d.
		hpCAD4	2.65 ± 0.88 (120)		**1.99 ± 0.16 (90)**	
		hpCAD19	**2.88 ± 0.98 (120)**		**1.99 ± 0.11 (90)**	
		hpCAD24	2.69 ± 0.83 (120)		1.95 ± 0.22 (90)	

Trees were scored in September 2014, September 2015 and September 2017. Incidence scores represent the level of infection or damage on the total leaf surface of the tree, while the severity scores represent the level of infection or damage on the most affected leaf. The data represent means ± SD. Values in bold font or underlined values indicate significantly increased or decreased values, respectively, as compared to those of the WT (Two-way ANOVA with Dunnett's post-hoc test; $P < 0.05$; n is indicated between brackets and represents biologically independent samples). n.d., not determined.

Table 5. Cell wall composition of field-grown *hpCAD* and WT poplars.

	H1 (2015)							H2 (2018)			
		red wood			white patch wood			main stem			
	WT	*hpCAD4*	*hpCAD19*	*hpCAD24*	*hpCAD4*	*hpCAD19*	*hpCAD24*	WT	*hpCAD4*	*hpCAD19*	*hpCAD24*
Cell wall composition											
CWR (% dry weight)	94.5 ± 0.7	94.4 ± 0.7	94.2 ± 0.7	94.4 ± 0.5	94.5 ± 0.6	94.1 ± 0.7	94.4 ± 0.8	92.2 ± 1.4	91.7 ± 1.4	91.0 ± 1.9	91.8 ± 1.5
Klason lignin (% CWR)	27.1 ± 3.2	24.8 ± 1.5	24.4 ± 2.2	24.2 ± 1.1	24.6 ± 2.6	24.7 ± 2.3	23.1 ± 1.2	25.1 ± 1.6	23.9 ± 1.9	25.3 ± 2.6	24.8 ± 2.9
Acid-soluble lignin (% CWR)	1.6 ± 0.1	1.6 ± 0.1	**1.7 ± 0.1**	1.6 ± 0.1	1.6 ± 0.1	1.5 ± 0.1	1.6 ± 0.2	1.7 ± 0.2	1.7 ± 0.2	1.7 ± 0.2	1.7 ± 0.2
Cellulose (% CWR)	43.0 ± 0.8	41.8 ± 0.6	41.8 ± 0.8	42.1 ± 0.6	**43.3 ± 1.5**	**43.0 ± 1.6**	**43.2 ± 2.1**[§]	42.6 ± 1.7	41.7 ± 1.2[§]	41.2 ± 1.5	41.6 ± 1.4
Hemicellulose (% CWR)	38.2 ± 2.0	**40.2 ± 1.3**	**39.6 ± 1.5**	**40.4 ± 1.3**	40.7 ± 1.2	38.8 ± 2.1	39.8 ± 2.6	39.9 ± 1.1	**41.7 ± 2.0**	**41.1 ± 1.5**[§]	**41.4 ± 1.4**
Relative distribution of main neutral sugars from amorphous polysaccharides (in mol%)											
Rha	3.44 ± 4.81	0.51 ± 0.07	0.53 ± 0.06	0.52 ± 0.08	0.45 ± 0.03	0.49 ± 0.08	0.48 ± 0.05	0.49 ± 0.07	0.44 ± 0.03[§]	0.47 ± 0.06	0.45 ± 0.04
Fuc	3.43 ± 4.95	0.41 ± 0.22	0.56 ± 0.06	0.53 ± 0.09	0.45 ± 0.04	0.33 ± 0.24	0.30 ± 0.21	0.50 ± 0.07	0.45 ± 0.03[§]	0.48 ± 0.06	0.45 ± 0.04
Ara	0.50 ± 0.07	**0.63 ± 0.16**	0.55 ± 0.09	0.58 ± 0.13	0.54 ± 0.06	0.55 ± 0.11	0.59 ± 0.09	0.54 ± 0.05	**0.66 ± 0.06**	**0.62 ± 0.04**	**0.62 ± 0.06**
Xyl	88.06 ± 9.45	**93.73 ± 1.55**	**93.73 ± 1.08**	**93.55 ± 1.89**	**94.06 ± 2.63**	92.31 ± 2.87	94.55 ± 1.14	93.34 ± 1.46	92.25 ± 1.30	93.64 ± 0.81	93.07 ± 1.36
Man	0.77 ± 0.32	1.14 ± 0.74	0.90 ± 0.49	0.77 ± 0.45	1.15 ± 1.05	1.57 ± 1.30	1.07 ± 0.70	0.72 ± 0.10	0.50 ± 0.07	0.50 ± 0.08	0.48 ± 0.05
Glc	2.02 ± 0.52	1.98 ± 0.72	2.02 ± 0.53	2.30 ± 1.06	1.79 ± 0.72	**2.80 ± 1.25**	1.89 ± 0.61	2.99 ± 0.74	**4.10 ± 1.22**	3.11 ± 0.56	3.44 ± 0.97
Gal	1.59 ± 0.31	1.60 ± 0.33	1.60 ± 0.37	1.63 ± 0.56	1.55 ± 0.47	1.64 ± 0.60	1.39 ± 0.11	1.43 ± 0.23	**1.77 ± 0.22**	**1.67 ± 0.25**	**1.64 ± 0.22**
Lignin composition											
H+G+S (µmol g^{-1} Klason lignin)	5441 ± 891	3818 ± 927	4275 ± 683	4071 ± 679	3784 ± 832	3889 ± 624	4035 ± 682	1521 ± 214	1299 ± 212	1252 ± 218	1309 ± 226
H (%)	0.46 ± 0.05	**0.75 ± 0.15**	**0.71 ± 0.10**	**0.71 ± 0.12**	0.72 ± 0.16	0.65 ± 0.08	0.78 ± 0.22	0.38 ± 0.06	**0.60 ± 0.20**	**0.66 ± 0.26**	**0.78 ± 0.46**
G (%)	27.36 ± 2.76	**32.13 ± 3.14**	**33.07 ± 2.72**	**33.20 ± 3.24**	32.51 ± 4.53	32.11 ± 1.90	33.33 ± 2.89	36.49 ± 1.00	37.03 ± 1.25	36.75 ± 1.69	37.46 ± 1.34
S (%)	72.18 ± 2.81	67.13 ± 3.26	66.22 ± 2.79	66.09 ± 3.34	66.76 ± 4.66	67.24 ± 1.89	65.89 ± 2.96	63.13 ± 1.04	62.38 ± 1.35	62.59 ± 1.89	61.76 ± 1.65
S/G	2.67 ± 0.35	2.12 ± 0.29	2.02 ± 0.23	2.02 ± 0.27	2.10 ± 0.39	2.10 ± 0.18	1.99 ± 0.22	1.73 ± 0.08	1.69 ± 0.09	1.71 ± 0.13	1.65 ± 0.10
Coniferaldehyde-derived dithioketal (µmol g^{-1} Klason lignin)	11.48 ± 4.50	6.81 ± 3.03	7.88 ± 1.89	7.80 ± 2.75	5.90 ± 2.41	5.73 ± 1.07	7.20 ± 2.11	1.12 ± 0.49	0.80 ± 0.29	0.83 ± 0.46	0.84 ± 0.36
Coniferaldehyde-derived indene (µmol g^{-1} Klason lignin)	b.d.l.	b.d.l.	b.d.l.	b.d.l.	b.d.l.	b.d.l.	b.d.l.	0.03 ± 0.02	**0.31 ± 0.09**	**0.31 ± 0.16**	**0.33 ± 0.11**
Sinapaldeldehyde-derived dithioketal (µmol g^{-1} Klason lignin)	2.97 ± 0.96	4.01 ± 2.63	**4.97 ± 1.77**	4.43 ± 2.30	4.12 ± 2.20	4.55 ± 1.54	5.94 ± 2.35	0.07 ± 0.03	**0.21 ± 0.10**	**0.26 ± 0.24**	**0.20 ± 0.12**
Sinapaldeldehyde-derived indene (µmol g^{-1} Klason lignin)	0.32 ± 0.20	**17.37 ± 7.80**	**21.27 ± 7.09**	**16.50 ± 7.16**	18.64 ± 9.06	17.11 ± 9.50	16.64 ± 7.42	0.16 ± 0.06	**5.96 ± 2.16**	**7.24 ± 4.20**	**7.31 ± 3.11**
Total Lignin-derived monomers (µmol g^{-1} Klason lignin)	5456 ± 895	3902 ± 954	4375 ± 703	4158 ± 700	3867 ± 855	3963 ± 644	4119 ± 704	1522 ± 215	1306 ± 213	1260 ± 222	1317 ± 228

Cell wall analyses of WT and red/white patch *hpCAD* wood derived from samples of the first harvest (H1) in 2015 and WT and *hpCAD* wood derived from the main stem of the second harvest (H2) in 2018. Cell wall residue (CWR) and its general composition are shown. The data represent means ± SD. Values in bold font or underlined values indicate significantly increased or decreased values, respectively, as compared those of the WT (for red *hpCAD* wood of H1 and *hpCAD* wood of H2) or red *hpCAD* wood of H1 (for white patch *hpCAD* wood of H1) (Two-way ANOVA with Dunnett's post-hoc test; $P < 0.05$; [§]$0.05 < P < 0.066$; n = 18 pools

(biologically independent samples were pooled three per three) per line for all WT and red *hpCAD* wood samples of H1; n = 18 biologically independent samples for the samples of H2; n = 19, 6 and 10 biologically independent white patch wood samples of *hpCAD4*, *hpCAD19* and *hpCAD24,* respectively). b.d.l., below detection limit. Remark: the data from H1 cannot be compared with the data from H2, as the samples were analyzed on different timepoints (using different batches of chemicals and sometimes different machinery, see materials and methods).

FIGURES AND FIGURE LEGENDS

Figure 1. Phenotype of field-grown *hpCAD* and WT poplars. (a) Photographs from growth and harvest 1. (Left) Picture of the field in February 2015. (Middle) Cross section of the stem showing the red xylem phenotype in (red and white patch) *hpCAD* poplars. In the red xylem of white patch *hpCAD* poplars, a white zone is present. (Right) Debarked stems from H1 showing the uniformly distributed red xylem phenotype in *hpCAD* poplars. (b) Photographs from growth and harvest 2. (Left) Picture of the field in August 2017. (Middle and right) Stem cross sections (middle) and debarked stems (right) from H2 showing the uniformly distributed red xylem phenotype in *hpCAD* poplars.

a

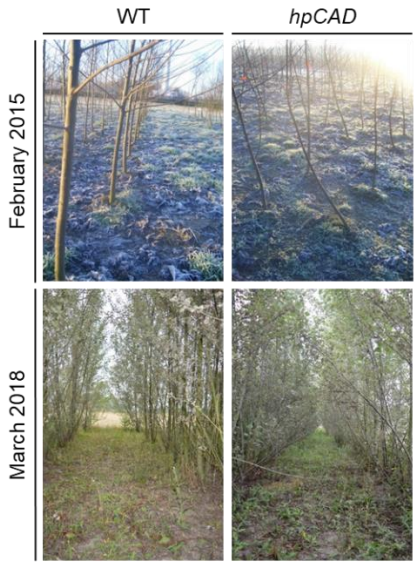

b

Harvest (year)	Line	Wood type	Leaning angle (°)	
H1 (2015)	WT	n.a.	3.99 ± 2.71	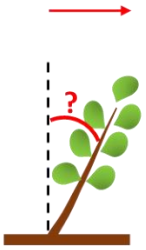
	hpCAD4	Red wood	**11.37 ± 6.63**	
	hpCAD19		**8.52 ± 5.58**	
	hpCAD24		**9.87 ± 6.15**	
	hpCAD4	White patch wood	**19.41 ± 5.50**	
	hpCAD19		**20.92 ± 5.21**	
	hpCAD24		**18.05 ± 7.43**	
Harvest (year)	**Line**	**Distance main stem and most outer branch (cm)**		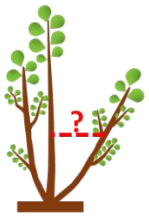
H2 (2018)	WT	53.60 ± 17.12		
	hpCAD4	**65.62 ± 21.13**		
	hpCAD19	**64.56 ± 19.16**		
	hpCAD24	**62.10 ± 17.75**		

Figure 2. Leaning phenotype of field-grown *hpCAD* poplars. (a) Picture of the trees showing the leaning phenotype in both one-year-old and three-year-old *hpCAD* lines. (b) Prior to the harvest (H1) in 2015, the leaning angle between a ruler perpendicularly positioned to the ground and every single tree was determined. The red arrow indicates the main wind direction, along which the *hpCAD* trees were leaning. Prior to the harvest (H2) in 2018, the distance between the main stem and the most outer branch per stool was measured at breast height. Values in bold font indicate significantly increased values as compared to those of the WT (for red *hpCAD* trees of H1 and *hpCAD* trees of H2) or red *hpCAD* trees of H1 (for white patch *hpCAD* trees of H1) (Two-way ANOVA with Dunnett's post-hoc test; $P < 0.05$; n = 240 biologically independent samples for WT of H1; n = 221 and 19 biologically independent *hpCAD4* samples for red and white patch trees, respectively, of H1; n = 234 and 6 biologically independent *hpCAD19* samples for red and white patch trees, respectively, of H1; n = 230 and 10 biologically independent *hpCAD24* samples for red and white patch trees, respectively, of H1; n = 160 biologically independent replicates for WT and *hpCAD4*, *hpCAD19*, *hpCAD24* of H2). n.a., not applicable.

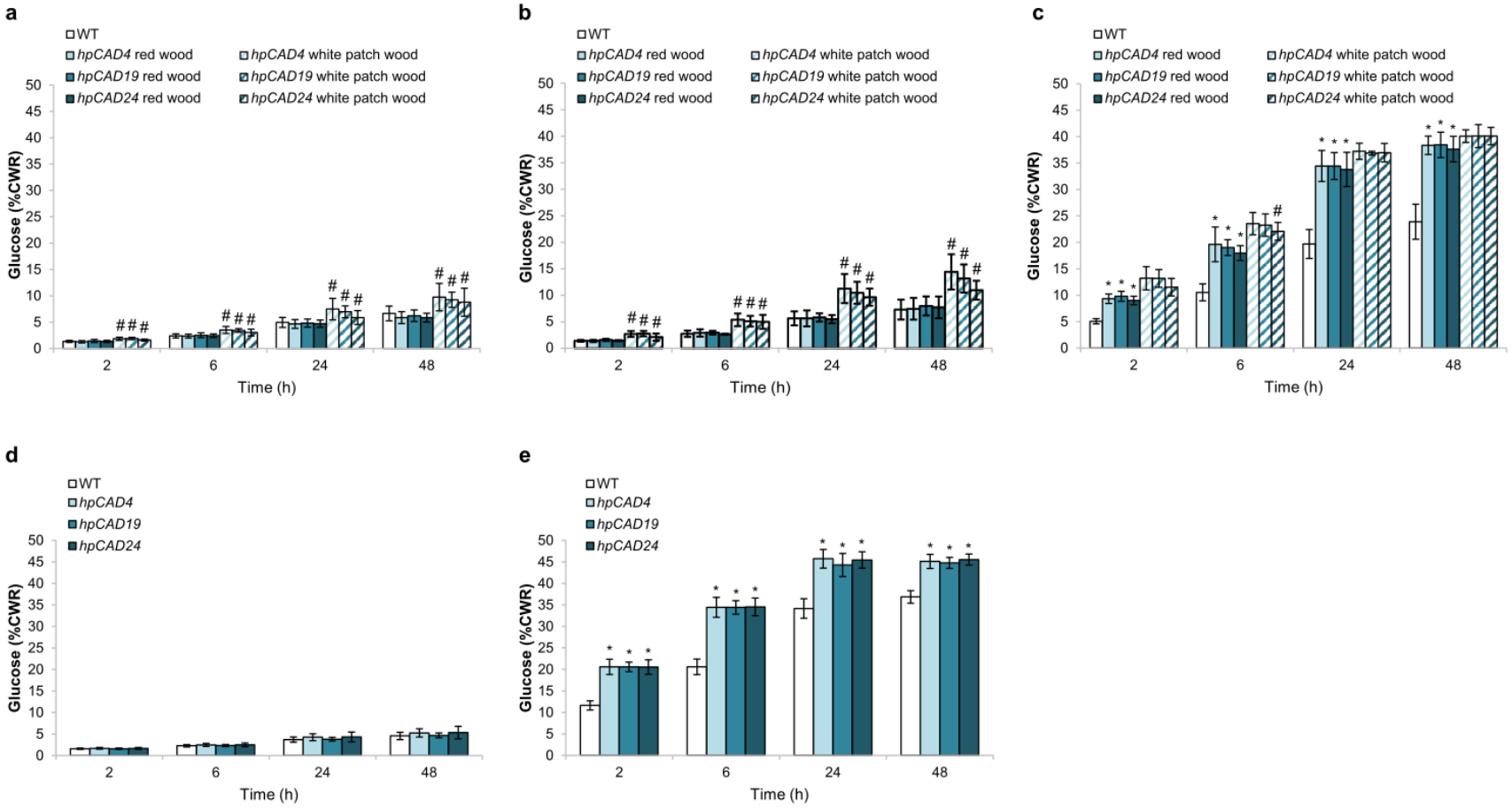

Figure 3. Saccharification assays of field-grown *hpCAD* poplars. (a-c) Saccharification yields of WT and *hpCAD* wood derived from H1. Glucose as %CWR after saccharification for 2, 6, 24 and 48 h using no (a), mild alkaline (6.25 mM NaOH) (b) or harsh alkaline (62.5 mM NaOH) (c) pretreatment. (d-e) Saccharification yields of WT and *hpCAD* wood derived from H2. Glucose as %CWR after saccharification for 48 h using no (d) or harsh alkaline (62.5 mM NaOH) (e) pretreatment. Bars represent means ± SD. *$P < 0.05$ (Two-way ANOVA with Dunnett's post-hoc test, comparisons made between red *hpCAD* and WT wood of H1 and *hpCAD* and WT wood from main stem of H2); # $P < 0.05$ (Two-way ANOVA with Dunnett's post-hoc test, comparisons made between white patch *hpCAD* wood and red *hpCAD* wood of H1); n = 18 per line for all (red) *hpCAD* and WT wood samples of H1 and H2; n = 19, 6 and 10 for the white patch wood samples of *hpCAD4*, *hpCAD19* and *hpCAD24,* respectively.